CHAPTER 119


NUMERICAL SIMULATION OF TURBULENT WAVE BOUNDARY LAYERS

J. H. Trowbridge[1], A.M.ASCE, C. N. Kanetkar[2] and N. T. Wu[3]

ABSTRACT: This paper reports numerical computations of fully rough turbulent boundary layers produced by first and second order Stokes waves. The computations are based on a mixing length turbulence closure and on a slightly more sophisticated turbulent kinetic energy closure. The first order results compare well with existing laboratory results. Reversal of the second order steady streaming under relatively long waves, which has been predicted analytically, is also predicted in the numerical results. The steady second order velocity field is found to become fully established only after a development time on the order of a few hundred wave periods. Both the first and second order results indicate that advection  and diffusion of turbulent kinetic energy play a minor role in determining the Reynolds averaged velocity field.

INTRODUCTION

        A quantitative understanding of turbulent wave boundary layers is necessary for coastal engineers concerned with dissipation of wave energy, wave-induced sediment transport, and the effect of waves on large-scale, slowly varying currents.  This study is confined to the case of fully turbulent boundary layers produced by weakly nonlinear waves near fixed hydrodynamically rough boundaries.  The boundary roughness elements are assumed to be small compared to the boundary layer thickness.

        Previous analytical studies (Kajiura, 1968; Grant and Madsen, 1979; Brevik, 1981; Myrhaug, 1982; Trowbridge and Madsen, 1984a), numerical studies (Bakker, 1974; Johns, 1975; Bakker and van Doorn, 1978), experimental studies (Jonsson, 1966; Jonsson and Carlsen, 1976; Bakker and van Doorn, 1978; Kamphuis, 1975) and semi-empirical analyses (Jonsson, 1966) have clarified the physics of the first-order problem. This is the purely oscillatory case corresponding to linear wave theory. By using relatively simple analytical solutions based on eddy-viscosity models, or numerical results based on Prandtl's mixing-length theory, one can predict with confidence the Reynolds-averaged velocity field, boundary shear stress and energy dissipation for the first-order case.

--------------------

[1]Assistant Professor, Dept. of Civil Engrg., University of Delaware, Newark, DE 19716.
[2]Central Water and Power Research Station, Pune, India.
[3]Graduate Student, Dept. of Civil Engrg., University of Delaware, Newark, DE 19716.

The second-order solution, which incorporates the effect of wave nonlinearity, is not as well established. The quantity of particular interest in the second-order problem is the steady streaming, or steady current which is generated in the boundary layer due to frictional dissipation of energy and nonlinearity. The asymmetry in the velocity field and bottom shear stress are also of interest in transport problems. Longuet-Higgins (1958) assumed that the effective viscosity is constant from the point of view of a moving fluid particle, although he allowed it to vary with mean particle position. He was able to show that under this restriction, the steady streaming just outside the wave boundary layer has the same value as in laminar flow. This value is independent of the molecular viscosity, and it is always in the direction of wave propagation. A later similar study, based on a time-invariant viscosity with a particular vertical structure, was reported by Johns (1970) with similar results. Later Johns (1977) reported a study based on a more realistic turbulent kinetic energy closure, but he neglected the second-order properties of the pressure field outside the boundary layer. In addition, he found that the steady streaming outside the boundary layer was zero. This result contradicts the laminar solution and existing analytical solutions, and will be discussed below in more detail. Trowbridge and Madsen (1984b) reported an analytical study based on a detailed, physically based eddy viscosity model, and found that the steady streaming produced by Stokes waves is in the direction opposite that of wave propagation for relatively long waves. Jacobs (1984) obtained a similar result by using an analysis based on Saffman's turbulence model.

Trowbridge and Madsen (1984b) found that their predictions of the steady streaming were sensitive to the eddy viscosity model. They used two models: one in which time variation of the viscosity extended throughout the boundary layer, and one in which the time variation of the viscosity was confined to a thin layer near the boundary. Example results are shown in Figure 1, indicating that predictions of the steady streaming are quite sensitive to the model used. The two models produced nearly indistinguishable results in the first order problem, and hence could not be judged on this basis.

Observations of the second-order properties of wave boundary layers are scarce. Bakker and Van Doorn (1978) reported a study carried out in a laboratory wave basin, in which the horizontal velocity was measured inside the boundary layer. In order to obtain turbulent flow at relatively small laboratory scales, Bakker and van Doorn had to use roughness elements which were quite large compared to the boundary layer thickness, and therefore the relevance for comparison with the theoretical studies quoted above is limited.

This paper reports a numerical study of turbulent wave boundary layers, based on Prandtl's mixing-length model and on a slightly more sophisticated turbulent kinetic energy closure, which was originally suggested by Prandtl (e.g., Schlichting, 1979), developed by several researchers, and summarized, for example, by Reynolds (1976). The purposes of this study are the following: (1) to clarify the physics of the second-order turbulent wave boundary layer; and (2) to give insight for developing a simpler analytical model which can be used as
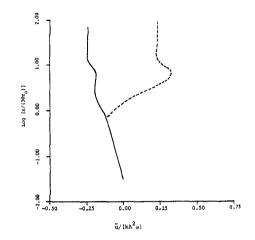
Figure 1.  Mean velocity $\bar{u}$ as a function of vertical coordinate z based on the analyses reported by Trowbridge and Madsen (1984b).  Solid line, first model; dashed line, second model.  kh = 0.50, $A/(30z_0)$ = 179.
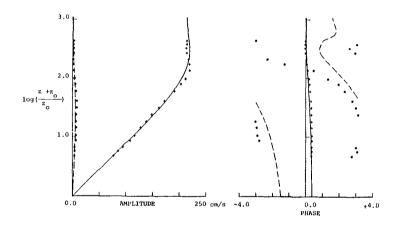


Figure 2.  Computed amplitude and phase of the first and third harmonics of the horizontal velocity based on the mixing length model, compared with measurements reported by Jonsson and Carlsen (Test 1).  Solid line, first harmonic; dashed line, third harmonic; asterisk, measurement.
$30\ z_0$ = 1.59 cm.

the basis for future studies involving more complicated processes.

GOVERNING EQUATIONS

     The flow to be considered is produced by a regular train of plane waves which is described locally by Stokes' second-order solution. The governing equations are the boundary layer approximation to the 2-D Reynolds-averaged mass and momentum equations. These are

$$\frac{\partial u}{\partial x} + \frac{\partial w}{\partial z} = 0 \tag{1a}$$

$$\frac{\partial u}{\partial t} + u \frac{\partial u}{\partial x} + w \frac{\partial u}{\partial z} = \frac{\partial U}{\partial t} + U \frac{\partial U}{\partial x} + \frac{\partial}{\partial z} \frac{\tau}{\rho} \tag{1b}$$

(e.g., Tennekes and Lumley, 1972) where x is the horizontal coordinate, positive in the direction of wave propagation, z is the vertical coordinate, positive upward with z equal to zero at the fixed bed, t is time, (u,w) is the Reynolds-averaged velocity vector inside the boundary layer, U is the horizontal velocity outside the boundary layer, $\tau$ is the Reynolds shear stress, and $\rho$ is the fluid density. The corresponding boundary conditions are the no-slip conditions at the bed and the no-stress condition far away from the bed:

$$u = w = 0 \qquad \text{at } z = 0 \tag{2a}$$

$$\tau \to 0 \qquad \text{as } z \to \infty \tag{2b}$$

The unsteady component of U is determined by Stokes' second-order solution, which is

$$U - \bar{U} = A \, \omega \, \cos(\omega t - kx) + \frac{3}{4} \frac{kA^2\omega}{\sinh^2(kh)} \cos[2(\omega t - kx)] \tag{3}$$

(e.g., Dean and Dalrymple, 1984). Here an overbar denotes a time-averaged quantity, A is the near-bottom excursion amplitude, $\omega$ is the radian frequency, k is the wave number, and h is the water depth. The steady component of U is determined by the mechanics of the boundary layer, and hence is not known initially.

     An additional equation necessary for the turbulence closure is the boundary layer approximation to the turbulent kinetic energy equation, which is

$$\frac{\partial}{\partial t} \left[ \frac{1}{2} q^2 \right] + u \frac{\partial}{\partial x} \left[ \frac{1}{2} q^2 \right] + w \frac{\partial}{\partial z} \left[ \frac{1}{2} q^2 \right] = \frac{\tau}{\rho} \frac{\partial u}{\partial z} + \frac{\partial D}{\partial z} - \epsilon \tag{4}$$

(e.g., Tennekes and Lumley, 1972) where $(1/2) \, q^2$ is the Reynolds averaged turbulent kinetic energy per unit mass, D is the vertical flux of kinetic energy due to turbulent "diffusion," and $\epsilon$ is the Reynolds averaged dissipation per unit mass.

     The leading terms in (1b) are the temporal acceleration terms and the stress term, and the leading terms in (4) are the time deriva-

tive term and the three terms on the right side (production, diffusion and dissipation). In both equations, the advective terms are order kA compared to the leading terms, and the neglected terms are order $k\delta$ compared to the leading terms, where $\delta$ is the boundary layer thickness. The viscous terms are neglected in both equations because they are small everywhere compared to the other terms for the case of hydrodynamically rough bed.

An important simplification is achieved by using the condition of periodicity in space and time. By using this condition together with the mass conservation equation to determine the vertical velocity, one can write equations (1b) and (4) as follows:

$$\frac{\partial u}{\partial t} - \frac{u}{c}\frac{\partial u}{\partial t} + \frac{1}{c}\frac{\partial u}{\partial z}\int_0^z \frac{\partial u}{\partial t}\,dz = \frac{\partial U}{\partial t} - \frac{U}{c}\frac{\partial U}{\partial t} + \frac{\partial}{\partial z}\left[\frac{\tau}{p}\right] \tag{5a}$$

$$\frac{\partial}{\partial t}\left(\frac{q^2}{2}\right) - \frac{u}{c}\frac{\partial}{\partial t}\left(\frac{q^2}{2}\right) + \frac{1}{c}\frac{\partial}{\partial z}\left(\frac{q^2}{2}\right)\int_0^z \frac{\partial u}{\partial t}\,dz = \frac{\tau}{\rho}\frac{\partial u}{\partial z} + \frac{\partial D}{\partial z} - \epsilon \tag{5b}$$

where c is the wave speed. Equations (5) involve derivatives with respect to z and t only, rather than x, z and t.

## TURBULENCE CLOSURES

We shall discuss results based on two turbulence closures. The first is Prandtl's mixing length model, which is

$$\tau = \rho\ \ell^2(z)\ \left|\ \frac{\partial u}{\partial z}\ \right|\ \frac{\partial u}{\partial z} \tag{6}$$

Here $\ell(z)$ is a vertical length scale which must by specified. We shall use simply

$$\ell = \kappa(z + z_0) \tag{7}$$

where $\kappa$ is the Karman constant and $z_0$ is the bed roughness scale. The turbulent kinetic energy equation is not needed for this closure, and the governing equations are simply (5a) and (6).

The second closure is a slightly more sophisticated turbulent kinetic energy closure. In this closure, the stress is written

$$\tau = c_2\ q\ \ell \tag{8}$$

where $c_2$ is an empirically determined constant, and the length scale $\ell(z)$ must be specified. As before, we shall use (7). The diffusion and dissipation terms are modeled by

$$D = c_2 \, c_3 \, q \, \ell \, \frac{\partial}{\partial z} \left[ \frac{q^2}{2} \right] \quad ; \quad \epsilon = c_1 \, q^3/\ell \qquad (9a)$$

where $c_1$ and $c_3$ are constants.  The boundary conditions for q are

$$q \to 0 \quad \text{as} \quad z \to \infty \quad ; \quad q^2 = c_4 \, |\tau/\rho| \quad \text{at} \quad z = 0 \qquad (9b)$$

where $c_4$ is an empirical constant.  The constants have been determined by other researchers by comparison with observations made in steady flows.   We shall use the following values:   $c_1 = 0.054$, $c_2 = 0.38$, $c_3 = 0.59$, $C_4 = 7$ (Reynolds, 1976).

It can easily be shown that the turbulent kinetic energy closure reduces to the mixing length model if temporal rate of change, advection, and diffusion of turbulent kinetic energy are neglected. The mixing length model can therefore be regarded as being based on a simplified turbulent kinetic energy balance in which production balances dissipation.

SOLUTION METHOD

As noted above, the advective terms on the left and right sides of (5a) and the left side of (5b) are order kA compared to the leading terms.   In Stokes waves, kA is a small quantity, and the advective terms may be neglected for the purpose of a first approximation, yielding

$$\frac{\partial u}{\partial t} - \frac{\partial}{\partial z} \left[ \frac{\tau}{p} \right] = \frac{\partial U}{\partial t} \qquad (10a)$$

$$\frac{\partial}{\partial t} \left[ \frac{q^2}{2} \right] - \frac{\partial D}{\partial z} - \frac{\tau}{\rho} \frac{\partial u}{\partial z} + \epsilon = 0 \qquad (10b)$$

These equations are consistent with Stokes first order solution (linear waves).   With the use of one of the turbulence closures discussed above, these equations may in principle be solved subject to the appropriate boundary conditions, with $\partial U/\partial t$ determined from the first term in (3).  This solution is purely oscillatory and contains only odd harmonics of the fundamental Fourier component, i.e., terms with periods of T, T/3, T/5,etc., where T is the fundamental wave period.

Once a first-order solution is obtained from (10), the small advective terms in (5) may be estimated from the first-order solution. Equations (5)can be written

$$\frac{\partial u}{\partial t} - \frac{\partial}{\partial z} \left[ \frac{\tau}{\rho} \right] = \frac{\partial U}{\partial t} - \frac{U}{c} \frac{\partial U}{\partial t} + \frac{u}{c} \frac{\partial u}{\partial t} - \frac{1}{c} \frac{\partial u}{\partial z} \int_0^z \frac{\partial u}{\partial t} \, dz \qquad (11a)$$

$$\frac{\partial}{\partial t} \left[ \frac{q^2}{2} \right] - D - \frac{\tau}{p} \frac{\partial u}{\partial z} + \epsilon = \frac{u}{c} \frac{\partial}{\partial t} \left[ \frac{q^2}{2} \right] - \frac{1}{c} \frac{\partial}{\partial z} \left[ \frac{q^2}{2} \right] \int_0^z \frac{\partial u}{\partial t} \, dz \qquad (11b)$$

With the advective terms determined by the first order solution, and with the terms involving U determined by both terms in (3), the right sides of equations (11) are known. By using one of the turbulence closures discussed above, one may in principle solve equations (11) subject to the appropriate boundary conditions. This procedure yields a solution consistent with Stokes' second order solution for the wave field. To this level of approximation, the boundary layer solution consists of a large, purely oscillatory, first order part, containing only odd harmonics of the fundamental Fourier component, and a smaller second order part, containing even harmonics of the fundamental Fourier component, as well as a steady component.

Equations (10) and (11) resemble coupled heat equations, each containing an unsteady term, a diffusion term, and various source and sink terms. These equations can be solved subject to the appropriate boundary conditions by means of a fully implicit, finite control volume procedure described in detail by Patankar (1980). In deriving this procedure, one integrates the governing equations across a small control volume of height $\Delta z$ and considers the fluxes of momentum and turbulent kinetic energy across the interfaces of each control volume. The scheme leads to a numerical time-stepping procedure in which one solves iteratively for the spatial distribution of velocity and kinetic energy at each time step.

In the computations described below, we used a vertical grid with a spacing varying as the cube of the distance above the solid boundary, and we applied the conditions at infinity at a finite distance above the boundary equal to A. In most computations we used 360 time steps per wave period and 51 grid points, and our convergence criterion was that the last iteration must yield values within approximately one part in $10^4$ of the previous iteration. We found that computations carried out on this basis yielded results which were nearly identical to results obtained with larger numbers of grid points and time steps, and with a stronger convergence criterion. We began the computations from rest, and we found that the first order solution reached a periodic state after roughly six to ten periods. The second order solution required a much larger time to reach a periodic state, as discussed below.

FIRST ORDER RESULTS

As discussed in the Introduction, the first order solution for the case of a fixed bed with roughness elements small compared to the excursion amplitude is fairly well established on the basis of existing experimental, theoretical and semi-empirical studies. The purposes of presenting additional first order results here are to show that the numerical solutions reproduce available observations, and to compare the results produced by the two different turbulence closures.

Figure 2 shows vertical distributions of amplitude and phase of the first two nonzero Fourier components in the first-order velocity field. The Figure also shows observations reported by Jonsson and Carlsen (1976, Test 1). The computations in Figure 1 are based on the mixing length closure. Figure 3 shows a comparison of results based
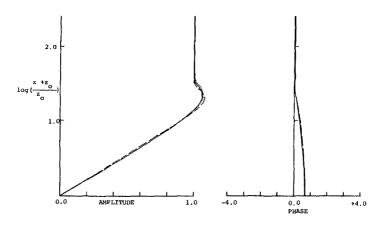
Figure 3.   Computed dimensionless amplitude and phase of the first
            harmonic of the horizontal velocity.   Solid line, mixing
            length model; dashed line, time rate of change of turbulent
            kinetic energy equal to production minus dissipation;
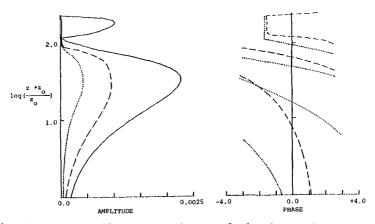            dotted line, turbulent kinetic energy closure.
            $z_0/A = 0.004$.



Figure 4.   Computed amplitude and phases of the first three nonzero
            Fourier components of the first order eddy viscosity,
            normalized by A and $\omega$, based on the mixing length model.
            Solid line, mean component; dashed line, second harmonic;
            dotted line, fourth harmonic.   $z_0/A = 0.004$.

on the mixing length model and on the turbulent kinetic energy closure. Both closures reproduce the experimental observations well, and the results based on the two closures are nearly indistinguishable from each other. A small improvement in the agreement between computations and observations is possible if one uses a more physically reasonable length scale than that given by (7). This point is well understood based on previous theoretical studies (Kajiura, 1968; Brevik, 1981; Trowbridge and Madsen, 1984a) and will not be pursued here.

We thought initially that because wave boundary layers are an unsteady phenomenon, the most important parts of the first-order turbulent kinetic energy balance might be unsteadiness, production and dissipation, because diffusion is known to be relatively small in steady turbulent flows near solid surfaces (e.g., Tennekes and Lumley, 1972). Neglect of the diffusion term in the turbulent kinetic energy balance leads to a simplified solution, because in this case no boundary conditions are necessary for the turbulent kinetic energy. We found, however, that computations based on a simplified model without the diffusion term are only slightly different, but slightly worse from the point of view of comparison with experiments, than computations based on either the mixing length or kinetic energy closures. We therefore abandoned this approach.

Figures 4 and 5 show computations of the eddy viscosity, $\nu_T$, which is defined by

$$\tau = \rho \ \nu_T \ \frac{\partial u}{\partial z} \tag{12}$$

In the mixing length closure,

$$\nu_T = \kappa^2 \ z^2 \ \left|\frac{\partial u}{\partial z}\right| \tag{13a}$$

and in the kinetic energy closure

$$\nu_T = c_2 \ q \ \ell \tag{13b}$$

The results in Figures 4 and 5 are very close. This is a convincing demonstration that the mixing length and kinetic energy closures give nearly identical results in the first order problem, because computations of eddy viscosity are more sensitive to the closure model than are computations of velocity.

The conclusions based on the first order results presented here are the following: (1) both turbulence closures reproduce the observations quite well; and (2) advection and diffusion of turbulent kinetic energy, which are the processes neglected in the mixing length model, have no significant effect on the Reynolds averaged motion.

SECOND ORDER RESULTS

Existing analytical models (Trowbridge and Madsen, 1984b) indicate that predictions of the second order boundary shear stress and the
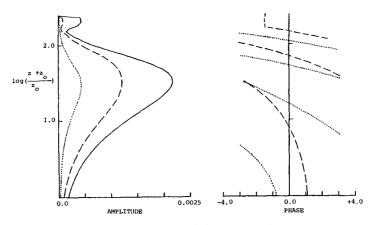
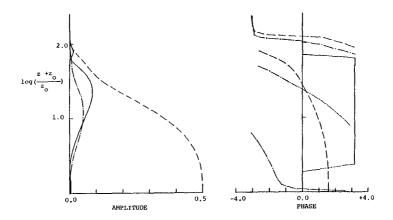Figure 5.   Computations as in Figure 4 based on the turbulent kinetic energy closure.



Figure 6.   Computed amplitudes and phases of minus the second order forcing term on the right side of (11a), normalized by $kA^2\omega^2$, based on the mixing length model.  Solid line, mean component;  dashed line, second harmonic;  dashed-dotted line, fourth harmonic.  $z_o/A = 0.004$, $kA = 0.2$, $kh = 1.0$.

unsteady component of the velocity inside the boundary layer are rela-
tively insensitive to the particular eddy viscosity model used.    In
discussing the second order results, we shall therefore concentrate on
the steady streaming.   Because there is no significant mean pressure
gradient in an oscillatory wave field, the steady motion is forced
solely by the nonlinear advective terms on the right side of equation
(11a).   In general, these terms contain a mean component plus compo-
nents at even harmonics of the fundamental frequency.   Figure 6 shows
the vertical distribution of the amplitudes and phases of the forcing
function on the right side of (11a).   The dominant forcing occurs at
twice the frequency of the first order wave field, but the mean forcing
is clearly evident.   Throughout most of the boundary layer, the mean
forcing is in the direction of wave propagation, but near the outer
edge of the boundary layer the mean forcing is in the opposite direc-
tion.   Outside the boundary layer, of course, the mean forcing is zero.

     In carrying out the second order solution, we began the computa-
tions from rest, as in the first order solution. The solution for the
velocity profile appeared to become nearly periodic after approximately
six to ten periods.   For those short times, we found mean velocity
profiles which approached zero outside the boundary layer, similar in
this respect to Johns' (1977) computations.   Computations carried out
over larger times, however, showed that the mean velocity inside the
boundary layer continues to evolve for a long period, gradually reach-
ing a steady state only after a few hundred periods.   Figure 7 shows
the mean velocity at several different times after the start of the
motion, indicating the gradual approach to a positive, steady profile
at very large times.   At small times, the velocity outside the boundary
layer is in the direction opposite that of wave propagation.   This
behavior is explained by the fact that the mean forcing is negative
near the outer edge of the boundary layer.   Initially, the boundary
layer thickness is small, and the vertical transport of momentum due
to Reynolds stresses is small compared to the mean forcing.   Conse-
quently, at small times the fluid at the outer edge of the boundary
layer acts like a frictionless fluid under the action of a mean,
negative, distributed body force.   The resulting velocity is negative
until the effect of the solid boundary diffuses outward far enough to
begin moving the fluid forward.   The results in Figure 7 are believed
to be qualitatively correct with possible quantitative discrepancies
due to recovery from initial conditions and the finite computational
domain.

     The velocities shown in Figure 7 correspond to kh equal to 1.0,
or waves in water of intermediate depth.   In this case, the mean
velocity at large times is in the direction of wave propagation.
Figure 8 shows similar mean velocity profiles for kh equal to 0.5,
corresponding to relatively long waves.   As in Figure 7, the gradual
approach of the mean velocity to a steady state is evident.   In Figure
8, however, the mean velocity is in the direction opposite that of wave
propagation.   This figure confirms qualitatively the reversal of the
steady streaming under long waves which was found analytically by
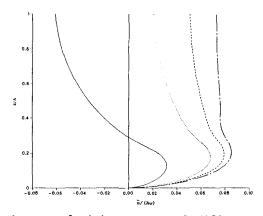Jacobs (1984) and Trowbridge and Madsen (1984b).

Figure 7. Computed mean velocities at several different times after the start of the motion. From left to right, the curves correspond to $t/T = 10$, $30$, $50$, $100$. $z_0/A = 0.004$, $kA = 0.2$, $kh = 1.0$.
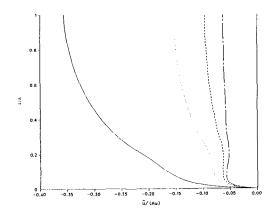


Figure 8. Computations as in Figure 7 for $kh = 0.5$.

Because of the long time periods required for the mean velocity to reach a steady state, numerical simulations of the second order problem based on implicit time-stepping procedures are very time-consuming. Our present results indicate, however, that computations based on the mixing length closure are nearly identical to computations based on the turbulent kinetic energy closure. Figures 7 and 8 are based on the mixing length model, and at relatively short times (of order ten wave periods) there is no significant difference between these results and the computations based on the turbulent kinetic energy closure.

The conclusions based on the second order computations are the following: (1) reversal of the steady streaming produced by relatively long waves is confirmed qualitatively; (2) the two turbulence closures give very similar results, indicating that processes in the turbulent kinetic energy equation other than production and dissipation have no significant effect on the Reynolds averaged velocity and stress; and (3) the time-averaged motion requires a very long time to reach a steady state. Conclusion (3) implies that the averaged motion may not become steady during time periods over which a natural wave field can be considered stationary. Consequently, it may be necessary to consider the history of the wave field when considering low frequency boundary layer motions produced by natural waves. In laboratory basins, where controlled, stationary conditions are possible for long times, the mean motion might have time to reach a steady state, if experiments are carried out for long enough periods.

A SIMPLE ANALYTICAL MODEL

For the purposes of studying more complicated processes, such as sediment transport, a simple analytical model which captures the main features of the flow is preferable to a more complicated, although possibly more consistent, numerical solution. One of the purposes of the numerical study reported here is therefore to guide development of realistic analytical models. The following very simple analysis is essentially the argument of Jacobs (1984) in a slightly more straight-forward form. It is based on a mean momentum balance derived by Longuet-Higgins (1958) and on the assumption of a constant friction factor.

The mean momentum balance derived by Longuet-Higgins (1958) is, to second order,

$$\bar{\tau}_b = -(\overline{uw})_{z=\infty} \tag{14}$$

where $\tau_b$ is the boundary shear stress. Use of the mass equation and the condition of periodicity in space and time shows that the vertical velocity may be written

$$w = \frac{1}{c} \int_0^z \frac{\partial u}{\partial t} \, dz \tag{15}$$

Substitution of the first order momentum balance (10a) yields

$$w = \frac{z}{c} \ \frac{\partial U}{\partial t} \ + \ \frac{1}{\rho c} \ (\tau - \tau_b) \tag{16}$$

to first order. Substitution of (16) into (14) and use of the boundary conditions (2) gives

$$\overline{\tau_b} = \frac{1}{c} \ \overline{\tau_b U} \tag{17}$$

correct to second order. If we assume that a constant wave friction factor f gives an adequate representation of the boundary shear stress, we have

$$\tau_b = \frac{1}{2} \ f \ \rho \ U|U| \tag{18}$$

Substitution of (3) and (18) into (17) yields, after straightforward algebra, the following result for the steady streaming just outside the boundary layer:

$$\overline{U} = \frac{2}{3} \ \frac{\overline{U^2}}{c} \ \left[ 1 - \frac{3}{4} \ \frac{1}{\sinh^2(kh)} \right] \tag{19}$$

correct to second order. Equation (19) is the result obtained by Jacobs (1984). This result agrees fairly well with the present numerical computations, and it indicates a reversal of the steady streaming produced by long waves. It is noteworthy that (19) is independent of the boundary roughness.

The above analysis may be used to calculate the time-varying boundary shear stress in a manner which incorporates the presence of the steady streaming consistently, although approximately.

REFERENCES

Bakker, W.T. 1974. *Proceedings of the 14th International Conference on Coastal Engineering*, ASCE.

Bakker, W.T. and van Doorn, Th. 1978. *Proceedings of the 16th International Conference on Coastal Engineering*, ASCE.

Brevik, I. 1981. *Journal of Waterway, Port, Coastal and Ocean Engineering*, *107*: 175-188.

Dean, R.G. and Dalrymple, R.A. 1984. *Water Wave Mechanics for Engineers and Scientists*, Prentice-Hall.

Grant, W.D. and Madsen, O.S.   1979.   Journal of Geophysical Research, 84: 1797-1808.

Jacobs, S.J. 1984.   Journal of Fluid Mechanics, 146: 303-312.

Johns, B.   1970.   Journal of Fluid Mechanics, 43: 177-186.

Johns, B.   1975.   Journal of Geophysical Research, 80:   5109-5112.

Johns, B.   1977.   Journal of Physical Oceanography, 7:   733-738.

Jonsson, I.G.   1966.   Proceedings of the 10th International Conference on Coastal Engineering, ASCE.

Jonsson, I.G. and Carlsen, N.A.   1976.   Journal of Hydraulic Research. 14: 45-60.

Kajiura, K.   1968.   Bulletin of the Earthquake Research Institute.   46: 75-123.

Kamphuis, J.W.   1975.   Journal of the Waterways, Harbors and Coastal Engineering Division, ASCE. 101: 135-144.

Longuet-Higgins, M.S.   1958.   Proceedings of the 6th International Conference on Coastal Engineering, ASCE.

Myrhaug, D.   1982.   Ocean Engineering, 9: 547-565.

Patankar, S.V.   1980.   Numerical Heat Transfer and Fluid Flow.   McGraw-Hill.

Reynolds, W.C.   1976.   Annual Review of Fluid Mechanics.   8:   183-208.

Schlichting, H.   1979.   Boundary Layer Theory.   McGraw-Hill.

Tennekes H. and Lumley, J.L.   1972.   A First Course in Turbulence. MIT Press.

Trowbridge, J.H. and Madsen, O.S.   1984a.   Journal of Geophysical Research.   89: 7989-7997.

Trowbridge, J.H. and Madsen, O.S.   1984b.   Journal of Geophysical Research.   89:   7999-8007.